An experimental study of the interaction of basaltic riverine particulate material and seawater

Journal Item

Available online at www.sciencedirect.com

SciVerse ScienceDirect

Geochimica et Cosmochimica Acta 77 (2012) 108–120

Geochimica et Cosmochimica Acta

www.elsevier.com/locate/gca

An experimental study of the interaction of basaltic riverine particulate material and seawater

Morgan T. Jones [a,b,*], Christopher R. Pearce [b,1], Eric H. Oelkers [b]

[a] Institute of Earth Science, University of Iceland, Sturlugata 7, 101 Reykjavik, Iceland

[b] GET, UMR CNRS 5563, Université Paul-Sabatier, Observatoire Midi-Pyrénées, 14 avenue Edouard Belin, 31400 Toulouse, France

Received 1 August 2011; accepted in revised form 28 October 2011

Abstract

The riverine transport of elements from land to ocean is an integral flux for many element cycles and an important climate regulating process over geological timescales. This flux consists of both dissolved and particulate material. The world's rivers are estimated to transport between 16.6 and 30 Gt yr^{-1} of particulate material, considerably higher than the dissolved flux of $\sim$1 Gt yr^{-1}. Therefore, the dissolution of particulate material upon arrival in estuaries and coastal waters may be a significant flux for many elements. Here we assess the role of riverine particulate material dissolution in seawater with closed-system experiments using riverine bedload material and estuarine sediment from western Iceland mixed with open ocean seawater. Both particulate materials significantly changed the elemental concentrations of the surrounding water with substantial increases in Si concentrations indicative of silicate dissolution. Seawater in contact with bedload material shows considerable enrichment of Ca, Mg, Mn, and Ni, while Li and K concentrations decrease. Moreover, the $^{87}Sr/^{86}Sr$ of seawater decreases with time with little change in Sr concentrations, indicative of a significant two-way flux between the solid and fluid phases. Mass balance calculations indicate that 3% of the Sr contained in the original riverine bedload was released during 9 months of reaction. In contrast, the estuarine material has a negligible effect on seawater $^{87}Sr/^{86}Sr$ and transition metal concentrations, suggesting that these reactions occur when particulate material first arrives into coastal waters. Solubility calculations performed using the PHREEQC computer code confirm that primary minerals are undersaturated, while secondary minerals such as kaolinite are oversaturated in the reacted fluids. These results demonstrate that riverine transported basaltic particulate material can significantly alter the composition of seawater, although the total concentrations of many major elements in seawater are regulated by the formation of secondary phases. This behavior has important implications for nutrient supply to coastal waters and the isotopic mass balance of several elements in the oceans.

1. INTRODUCTION

Riverine transport from the continents to the oceans is a major process in the global cycling of the elements. In many instances this transport plays a critical role in other processes. For example, it has been argued that the riverine transport of Ca and Mg to the oceans is the most important climate regulating process over geological timescales (Walker et al., 1981; Berner et al., 1983; Berner, 1990; Kump et al., 2000; Gislason et al., 2006). Riverine transport of key nutrients (e.g. N, P, Ca, Mg, Si, Fe, Mn, Zn) is also essential to marine primary productivity (Holland, 1984; Falkowski, 1997; Falkowski et al., 1998; Mörner and Etiope, 2002; Holland, 2005). The transport of radiogenic isotopes, such as Sr and Nd (Raymo et al., 1988; Burton and Vance, 2000; Andersson et al., 2001), and stable isotopes such as Li, Mg and Si (De La Rocha et al., 1997; Huh et al., 2001; Kisakürek et al., 2005; Villiers et al., 2005; Georg et al., 2007; Wimpenny et al., 2010), are

* Corresponding author at: Institute of Earth Science, University of Iceland, Sturlugata 7, 101 Reykjavik, Iceland.
E-mail address: morgan@hi.is (M.T. Jones).
[1] Present address: Department of Earth and Environmental Sciences, The Open University, Walton Hall, Milton Keynes MK7 6AA, United Kingdom.

0016-7037/$ - see front matter © 2011 Elsevier Ltd. All rights reserved.
doi:10.1016/j.gca.2011.10.044

integral to the understanding of global biogeochemical and element cycles.

The world's rivers transport material from the land to the oceans in dissolved form, a product of chemical weathering, and as particulate matter from mechanical weathering and the growth and decay of organic material. Dissolved riverine transport has received much greater attention than riverine particulate material, both in the fluxes of elements to the oceans and the climatic implications (Gislason et al., 2006). Based on the water chemistry and fluxes of the world's major rivers, the global dissolved riverine flux is estimated to be approximately 1 Gt yr^{-1} (Gaillardet et al., 1999, 2003; Viers et al., 2009). Global sediment fluxes are somewhat more difficult to quantify due to damming of rivers, data reliability issues, an absence of bedload information on many rivers, many ungauged rivers, uncertainties regarding the proportion of sediment that reaches the ocean, and the huge fraction of particulate material transported during flood events (Walling, 2006; Syvitski, 2011). Moreover, estimates of riverine fluxes are commonly derived from spot samples that are applied over a longer time period. Particulate transport is more strongly dependent on weather than dissolved transport and can vary hourly (Gislason et al., 2006, 2008). Most particulate matter flux estimates are restricted to suspended material, which are estimated to have land-to-ocean fluxes of 15–20 Gt yr^{-1} (Meybeck et al., 2003; Syvitski, 2003; Syvitski et al., 2003; Walling, 2006; Peucker-Ehrenbrink et al., 2010). Bedload fluxes are also difficult to quantify; calculations based on lost reservoir storage and GIS measurements suggest an annual sediment trapping of 4–25 Gt yr^{-1} (White, 2001; Vörösmarty et al., 2003). If it is assumed that 40% of this material evades sedimentary traps and reaches the ocean, then there is an additional global bedload flux of 1.6–10 Gt yr^{-1} (Walling, 2006). This additional bedload flux would increase the total land to ocean global particulate flux estimate to 16.6–30 Gt yr^{-1}.

These overall flux estimates illustrate that the mass transport of particulate material is at least an order of magnitude greater than the dissolved riverine transport of material to the oceans. The importance of particulate riverine transport varies significantly between elements due to their distinct solubilities in river water. The relative fluxes of suspended particulate material and dissolved species of elements to the oceans are shown in Fig. 1. Suspended material fluxes dominate over dissolved fluxes for the majority of elements (Oelkers et al., 2011). Of the metals, only Na is greater in the dissolved flux, all others are dominated by suspended material transport. For soluble elements such as Li, Mg, Ca, and Sr, suspended material transport is less than an order of magnitude greater than dissolved transport. For insoluble elements such as Al, Ti, Fe, and Zr, however, suspended material transport fluxes exceed dissolved material fluxes to the oceans by more than a factor of 1000 (Gaillardet et al., 1999, 2003; Viers et al., 2009). Note that these comparisons are based only on the mass of suspended material transport; total riverine particulate transport to the oceans also includes the contribution

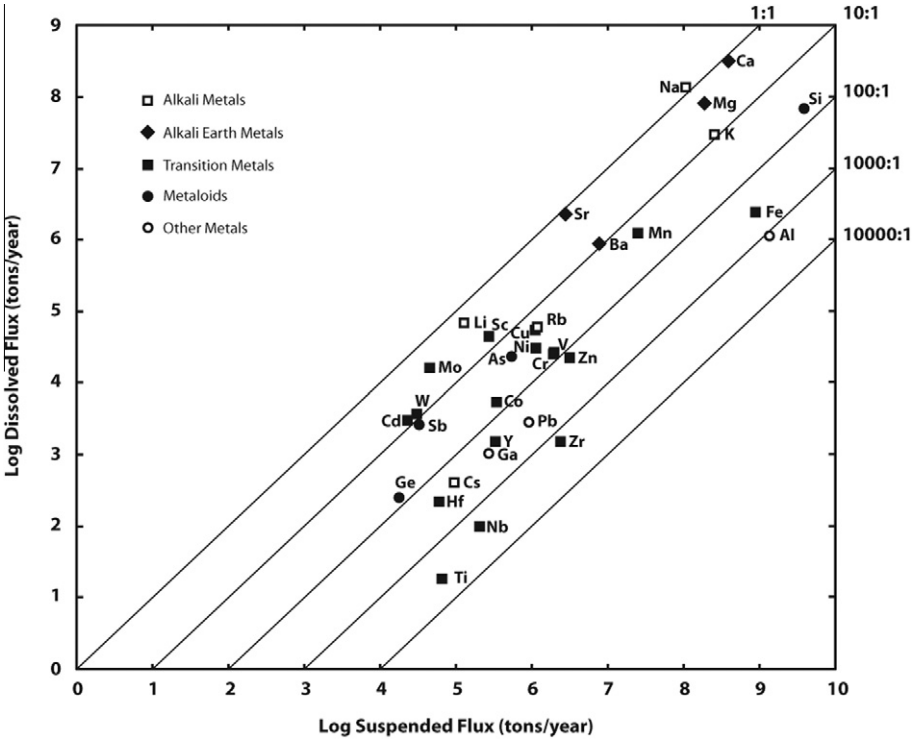

Fig. 1. The ratio of suspended flux to dissolved flux for selected elements transported from the continents to the oceans worldwide (Gaillardet et al., 1999, 2003; Viers et al., 2009). These flux estimates are from comprehensive studies of global rivers and can therefore be considered for direct comparison.

of bedload transport, which would further increase the dominance of particulate over dissolved transport.

The degree to which this particulate matter plays a role in the compositional evolution of seawater depends on its dissolution rate after it arrives in the ocean. The world's deltas and estuaries act like fluidized bed reactors and are periodically reworked for days to months after arrival from fluvial systems (Aller, 1998), so there is considerable time for interaction between particulate matter and seawater prior to deep burial. This interaction between deposited particulate matter with saline pore fluids leads to a series of diagenetic reactions that has been referred to in the literature as reverse weathering (Mackenzie and Garrels, 1966; Michalopoulos and Aller, 1995; Zhu et al., 2006; Aller et al., 2008; Dürr et al., 2009). Oelkers et al. (2011) concluded that a Si dissolution rate of 1×10^{-16} mol cm^{-2} s^{-1} is sufficient to dissolve 1% of the riverine transported particulate material to the oceans annually. Of the particulate material that arrives to the ocean, the more reactive fraction originates from volcanic islands (Oelkers and Gislason, 2004; Wolff-Boenisch et al., 2004, 2006). This fraction constitutes up to 45% of the total suspended flux globally (Milliman and Syvitski, 1992). Basaltic glass dissolution rates at the pH and temperature range of ocean waters suggests that ~0.05% of basaltic suspended material would dissolve in seawater each day (Oelkers and Gislason, 2001; Gislason and Oelkers, 2003; Jones and Gislason, 2008). Even basaltic glass that is already severely weathered continues to dissolve when exposed to seawater (Stefánsdóttir and Gislason, 2005). Gislason et al. (2006) and Wallmann et al. (2008) concluded that the particulate flux of Ca that subsequently dissolves in seawater is comparable to that derived from the dissolved flux. Tracing and understanding these contributions will constrain the current understanding of ocean circulation, biological productivity, and element cycling (Jeandel et al., 2011). This study aims to further illuminate the role of riverine transported particulate material to the oceans on the global cycles of the elements through the direct measurement of elements liberated to seawater from particulate material dissolution.

2. MATERIALS AND METHODS

2.1. Sampling localities and methods

This study focuses on the reactivity of particulate samples obtained from the Hvítá River and the Borgarfjörður Estuary in western Iceland (Fig. 2). Several studies have previously focused on the major element and isotope systematics of this river and estuary system (Gislason et al., 1996; Gannoun et al., 2006; Pogge von Strandmann et al., 2006, 2008a,b, 2011; Vigier et al., 2006; Georg et al., 2007; Vigier et al., 2009; Pearce et al., 2010). These studies provide the basis for understanding the interaction between riverine particulate material and seawater in this study. Iceland is ideal for identifying particle–fluid interactions for a number of reasons. First, the dominantly homogeneous basaltic geology of Iceland allows for the elimination of lithological variability from weathering processes. Second, there is a low biological influence as vegetation is comparatively sparse and soils are poorly developed. Third, the oceanic boreal climate is well characterized, with a mean annual temperature of 4 °C and a seasonal variability of ±15 °C (Eythorsson and Sigtryggsson, 1971; Saemundsson, 1979; Gislason et al., 1996). The mean annual precipitation at these western Iceland sampling sites is estimated to be between 770 and 1000 mm a^{-1} (Eythorsson and Sigtryggsson, 1971; Georg et al., 2007; Pogge von Strandmann et al., 2008b).

The Hvítá River catchment covers approximately 1685 km^2 and consists of mostly basaltic rock with some minor felsic outcrops, all younger than 3.3 Ma (Gislason et al., 1996; Tronnes, 2003). To the eastern part of the catchment is the Langjökull icecap, so part of the

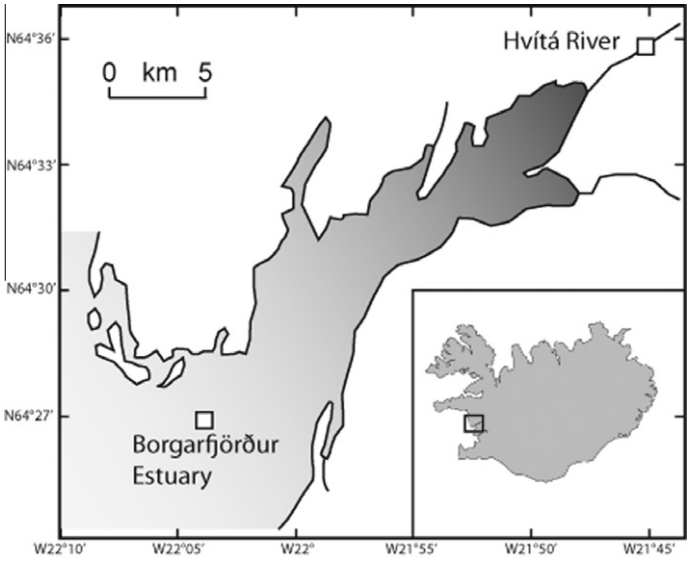

Fig. 2. A map of Borgarfjörður Estuary in western Iceland, showing the sample locations used in this study.

transported particulate material is tilled. Glacial dominated tributaries and spring-fed tributaries often have a high pH due to isolation from atmospheric CO_2. Hvítá River has both spring and glacial components, and the pH measured close to the mouth of the river is between 7.70 and 7.93 (Georg et al., 2007; Pogge von Strandmann et al., 2008a; Pearce et al., 2010). Physical erosion and chemical weathering rates are estimated at 1090 and 72 t km^{-2} yr^{-1}, respectively (Pogge von Strandmann et al., 2006). The Borgarfjörður Estuary is over 25 km long and up to 5 km wide. It is <2 m deep for the first 5 km from the river mouth but then increases rapidly to a depth of around 100 m after 10 km. The river discharge is low, leading to a tide-dominated estuary that is both vertically and horizontally well mixed.

Bedload material from the Hvítá River was collected from a sandbank immediately adjacent to the main flow. Three kilograms of material was collected and split between 1 L plastic containers. The sampling location (see Fig. 2) was at the confluence of the catchment (i.e. it includes contributions from the Norðurá and Grimsá tributaries), but before the start of the Borgarfjörður Estuary. Estuarine sediment was collected ~29 km away from the Hvítá River particulate sample site, near the center of the Borgarfjörður Estuary mouth (see Fig. 2). This site is approximately 20 km from the mixing zone at high tide, and therefore the coexisting brine is dominated by seawater. Temperature, pH, salinity, and elemental concentrations demonstrate that the overlying water-column has a predominantly marine composition at this distance (Pogge von Strandmann et al., 2008b; Pearce et al., 2010). Surface sediment was collected at a water depth of ~100 m using a weighted bucket dragged behind a boat over a distance of ~10 m. Three repeat passes yielded >3 kg of material that was homogenized and split into three separate sample pots. All solids were dried at 40 °C immediately after collection but no other processing was done. The open-ocean surface water used in the closed system experiments was collected from the sub-tropical North Atlantic Ocean during the TOPOGULF cruise. The water represents an amalgamation of surface water collected from the central gyre and is consequently low in dissolved silica (0.28 ppm Si). Open-ocean seawater was chosen for this study as an end member of fluids present in the mixing zone. Moreover the use of open-ocean seawater allows a clearer identification of the effects of particulate–fluid interaction than the brackish estuarine waters that have already interacted with particulates in the natural environment. The water was acidified to pH 2 using 7 M HCl upon collection and was subsequently stored in the dark. Prior to commencing the experiments the pH was re-equilibrated to 8.1 at 21 °C using 1 M NaOH.

Table 1
The BET surface areas, bulk compositions, $^{87}Sr/^{86}Sr$ isotopic ratios, and mineralogical assemblage of the samples before the experiments. Assemblages were estimated by grain counting using Scanning Electron Microscopy.

	Borgarfjörður Estuary	Hvítá River
BET (m^2 g^{-1})	7.357	6.358
SiO_2 (%)	40.71	46.74
Na_2O (%)	2.9	2.67
MgO (%)	8.52	8.17
Al_2O_3 (%)	12.83	15.24
P_2O_5 (%)	0.19	0.14
K_2O (%)	0.45	0.28
CaO (%)	15.7	14.02
TiO_2 (%)	2.44	1.45
MnO (%)	0.26	0.24
$Fe_2O_3^*$ (%)	14.41	10.81
Sr (mg kg^{-1})	271.1	152.9
$^{87}Sr/^{86}Sr$	0.70629	0.70318
Microcrystalline (%)	50.25	55.07
Volcanic glass (%)	18.23	18.94
Ca feldspar (%)	10.84	10.57
Olivine (%)	7.39	7.93
Fe–Ti oxides (%)	4.93	4.41
K feldspar (%)	2.46	2.64
Quartz (%)	1.48	0.44
Calcite (%)	4.43	0

* Denotes total iron.

The specific Brunauer Emmett Teller (BET) surface area, major elemental composition, and mineralogy of the particulate material are shown in Table 1. The mineralogy of the samples was determined by counting ~300 grains using a Scanning Electron Microscope (SEM). The olivines present had a typical composition of $Mg_{1.6}Fe_{0.4}SiO_4$ (forsterite > fayalite), although the SEM analysis suggested significant H_2O was present, indicative of partial alteration to phyllosilicates. The feldspars fell into two distinct categories, bytownite ($\sim Na_{0.2}Ca_{0.8}Al_{1.8}Si_{2.2}O_8$) and anorthoclase ($\sim Na_{0.7}K_{0.2}Ca_{0.1}Al_{1.1}Si_{2.9}O_8$). Both the micro-crystalline material and volcanic glass had compositions close to the bulk sample. The mean grain sizes for the samples, as determined by SEM analysis, are ~200 μm for the Hvítá riverine bedload and ~75 μm for the Borgarfjörður estuarine sediment. Despite the difference in grain size, the two samples exhibit comparable BET surface areas, mineralogy, and bulk compositions, with the exception of the presence of minor calcite in the Borgarfjörður Estuary sample (see Table 1). The presence of calcite in the Borgarfjörður Estuary sample is consistent with the dominance of seawater in the brine present at this sampling locality; note that seawater is supersaturated with respect to calcite.

2.2. Experimental methods

Closed-system experiments were performed by reacting bedload material from Hvítá River and surface sediment from the Borgarfjörður Estuary with open-ocean seawater. In total, four closed system experiments were performed. Two experiments were performed with Hvítá River bedload material; one at 5 and the other at 21 °C. Corresponding experiments were also performed on the Borgarfjörður Estuary surface sediment. Each experiment used 250 g of particulate material and 900 ml seawater and ran for a period of 9 months. The reactors were periodically sampled, taking 30 ml aliquots of fluid through a 0.22 μm filter. This sample was divided; one sub-sample was used for pH measurements and the second for elemental analysis. The reactors were manually shaken weekly and after each sampling. The removal of samples lowered the fluid volume by ~25% during the experiments.

Element analysis for both particulate and water samples were conducted using an Agilent 7500 quadruple inductively coupled plasma mass spectroscopy (Q-ICP-MS). Samples of the original particulate material were dissolved first using 1 ml HNO_3 and 1 ml HF, evaporated, then attacked again using 2 ml HCl and 1 ml HNO_3 (aqua-regia) prior to analysis. This digestion procedure resulted in complete dissolution of the particulate samples. An In Re spike was used for calibration purposes and total blank contributions were negligible compared to sample concentrations. Uncertainties determined using replicate samples and standard measurements did not exceed ±5%, except where element concentrations were below detection limits (see Table 2), or where there was very high initial concentrations in the seawater (e.g. Na). Silica concentrations in the solid samples were determined using a fusion method and using inductively coupled plasma atomic emission spectroscopy (ICP-AES). Silica concentrations in the fluid samples were ascertained by colorimetry on a Technicon auto-analyzer using the Molybdate Blue method (Koroleff, 1976). The error on this method is ±4%.

The $^{87}Sr/^{86}Sr$ ratios for each sample were measured using a VG Sector 54 thermal ionization mass spectrometer (TIMS). Samples were evaporated, taken up in 3 M HNO_3 and run through Sr-spec columns. The purified Sr was then loaded onto outgassed Ta filaments. The samples were run at ^{88}Sr beam potentials of 2 V and 100 ratios were collected using a multi-dynamic peak jumping routine. Resulting $^{87}Sr/^{86}Sr$ ratios were normalized to an $^{86}Sr/^{88}Sr$ ratio of 0.1194. Six analyses of the NBS 987 standard yielded an average $^{87}Sr/^{86}Sr$ of 0.710232 ± 0.000011 (2 SD). The commonly accepted literature value is 0.710263 ± 0.000016 (Stein et al., 1997). Individual errors did not exceed ± 0.000017 $^{87}Sr/^{86}Sr$. Total blanks (acid digestion, column chemistry) for Sr were found to be negligible compared to the Sr amounts from the samples.

The thermodynamic calculations presented in this study were performed using the PHREEQC computer code (Parkhurst and Appelo, 1999). The database used was phreeqc.dat, with additional thermodynamic data on magnesite, siderite, thomsonite, scolecite, mesolite, laumontite, heulandite, analcime, Ca-stilbite, Ca-mordenite, Ca-clinoptilolite, Fe-celadonite, antigorite, amorphous SiO_2, amorphous FeOOH, amorphous $Al(OH)_3$, gibbsite, allophane, and imogolite taken from previous studies (Gysi and Stefansson, 2008; Gudbrandsson et al., 2011). All computer models assumed saturation with respect to atmospheric CO_2 and O_2 at the measured temperature and pH.

3. RESULTS

3.1. Element release during dissolution

Dissolution of both the bedload material from the Hvítá River and estuarine sediment from Borgarfjörður significantly changed the elemental concentrations of the surrounding seawater. The temporal variation of selected major element concentrations in seawater is shown in Fig. 3, while the complete range of measured element concentrations and $^{87}Sr/^{86}Sr$ values of the reacted fluids are shown in Table 2.

The concentrations of dissolved Si in seawater increase markedly in all four experiments, indicating the dissolution of primary silicate material. The greatest change in concentration occurs in the Hvítá bedload experiment at 21 °C, where the Si concentration rises from 0.28 to 6.18 ppm (see Fig. 3). This concentration subsequently decreases over time, although it remains relatively high at the end of the experiment (4.8 ppm). The smallest change in Si concentration occurs in the Borgarfjörður sediment experiment at 5 °C, reaching 2.89 ppm by the end of the experiment. Temperature has a greater effect on Si release than the identity of the sample.

Other elements show considerable enrichment in seawater during the experiments. In particular, Mn and Ni are considerably enriched in seawater when reacted with the Hvítá River bedload (Fig. 3), similar to previous work on weathered basaltic glass/seawater experiments (Stefánsdóttir and Gislason, 2005). Manganese concentrations increase to 0.8 and 2 ppm at 5 and 21 °C, respectively, in the Hvítá River bedload experiments. Unlike Si, the behavior of Mn and Ni in the Borgarfjörður estuarine sediment experiments contrasts with that of the Hvítá bedload experiments. Although Mn initially increases it rapidly falls below detection in the Borgarfjörður estuarine sediment experiments. Dissolved Ni increased in all experiments, although to a greater extent in the Hvítá River bedload experiments, increasing from 0.1 to >10 ppb at both temperatures. Other measured transition metals (Cu, Zn, and Mo) show various differences in behavior between the bedload and estuarine samples, but these numbers are close to or below the detection limit (see Table 2). The concentrations of Fe, both in the original seawater and all reacted samples, remained below the analytical detection limit of 20 ppb.

There is a significant difference in the alkali metal release rates to seawater between the estuarine and riverine samples. The high concentrations of Na in seawater prevented accurate measurements of any changes in concentration. Both Li and K, however, decrease in the seawater reacted with Hvítá River bedload material. In the case of Li the decrease is substantial, dropping from >150 to <50 ppb at both temperatures (Fig. 3). In the case of K the decrease in seawater concentrations are less pronounced, although this is likely due to the abundance of K in seawater. In contrast, seawater in contact with Borgarfjörður estuarine material displays slight increases of Li and K at both 5 and 21 °C. Therefore, unlike the Si release, the behavior of alkali metals appears dependent on whether the material has already been exposed to saline water.

The alkali earth metals, namely Mg, Ca, Sr, and Ba, also show temporal concentration variations throughout each experiment. These elements are generally enriched in seawater when reacted with the Hvítá riverine bedload material, especially Ba (Fig. 3). Mg and Ca also show measureable increases greater than the statistical error, while Sr fluctuates near the original seawater composition (Table 2). The seawater reacted with estuarine material from Borgarfjörður displays a large increase in Mg, Ca,

and Sr concentrations. In contrast to the Hvítá bedload material, the increase in Ba concentrations is minimal (Fig. 3).

Solubility calculations were performed using the PHREEQC computer code (Parkhurst and Appelo, 1999) to assess the saturation states of various minerals; the

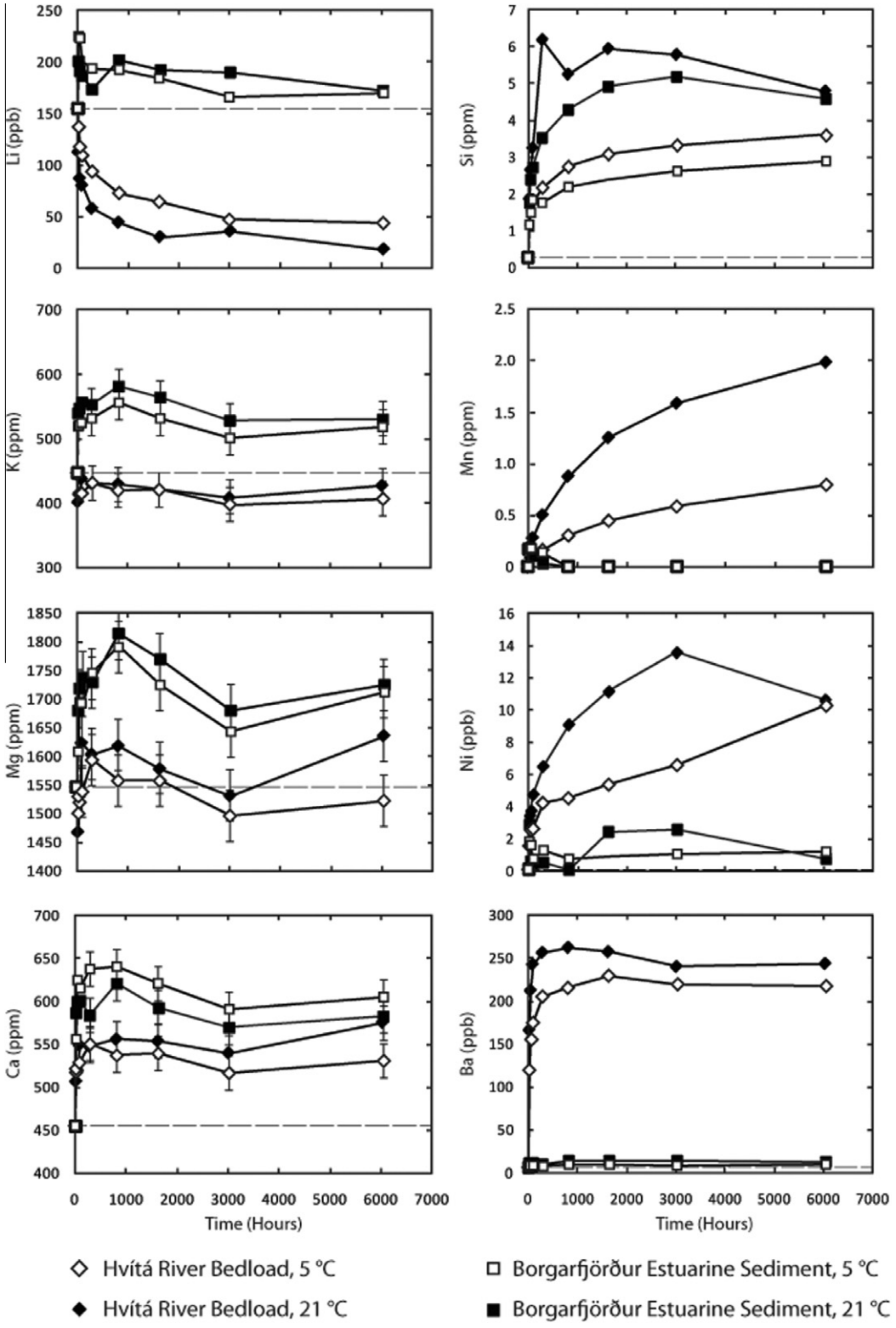

Fig. 3. The concentrations of selected elements in seawater when mixed with basaltic riverine and estuarine material in closed-system batch reactors. The dashed lines indicate the concentrations in the original seawater. Error bars are shown for K, Mg, and Ca, for all other elements the errors are within the size of the symbols.

Table 2
The measured concentrations of measurable elements and $^{87}Sr/^{86}Sr$ values in seawater during the experiments.

Units	Sample	No.	Tempera-ture Celsius	Time Hours	Time Months	Mass solid grams	Mass fluid grams	pH	Si ppm	Li ppb	B ppm	Mg ppm	Al ppb	K ppm	Ca ppm	Mn ppb	Ni ppb	Rb ppb	Sr ppm	Cu ppb	Ba ppb	Zn ppb	Mo ppb	U ppb	$^{87}Sr/^{86}Sr$
	Hvítá	0	5	0	0	250.1	895.9	8.13	0.28	155	5.16	1546	181	447	455	*0*	*0.1*	130	8.85	*0*	7	39	13	3.4	0.709155
	Hvítá	1	5	22	0.03	250.1	865.9	7.53	1.16	138	4.68	1500	190	414	521	104	*1.6*	137	8.65	*3*	120	63	11	*0.3*	0.708909
	Hvítá	2	5	49	0.07	250.1	835.9	7.10	1.53	117	4.51	1520	221	414	519	122	*2.6*	133	8.73	3	156	39	10	*0.1*	0.708827
	Hvítá	3	5	92	0.13	250.1	805.9	6.95	1.76	109	4.55	1538	184	416	529	130	*2.7*	134	8.79	3	175	47	10	*0.0*	0.708789
	Hvítá	4	5	291	0.40	250.1	775.9	6.67	2.17	94	4.57	1594	183	430	550	171	4.2	138	9.16	*3*	205	44	9	*0.0*	0.708713
	Hvítá	5	5	816	1.13	250.1	745.9	6.61	2.75	72	4.44	1558	149	420	538	306	4.6	135	9.02	*3*	216	43	8	*0.0*	0.708619
	Hvítá	6	5	1632	2.27	250.1	715.9	6.70	3.09	64	4.44	1558	169	421	540	450	5.4	137	9.04	*3*	230	55	6	*0.0*	0.708564
	Hvítá	7	5	3018	4.19	250.1	685.9	6.68	3.33	48	4.25	1496	142	398	516	589	6.6	131	8.78	*2*	220	41	5	*0.0*	0.708482
	Hvítá	8	5	6042	8.39	250.1	655.9	6.65	3.61	44	4.29	1522	181	407	531	798	10.3	133	8.80	*3*	217	54	5	*0.0*	0.708472
	Borgarfjörður	0	5	0	0	254.3	858.1	8.13	0.28	155	5.16	1546	181	447	455	*0*	*0.1*	130	8.85	*0*	7	39	13	3.4	0.709155
	Borgarfjörður	1	5	22	0.03	254.3	828.1	8.11	1.21	224	4.89	1613	*37*	519	557	176	*1.9*	212	10.20	13	10	21	17	0.3	n.a.
	Borgarfjörður	2	5	49	0.07	254.3	798.1	8.07	1.48	222	4.88	1694	64	524	625	160	*1.5*	175	11.07	21	8	31	16	0.3	n.a.
	Borgarfjörður	3	5	92	0.13	254.3	768.1	8.04	1.82	201	4.89	1688	67	525	615	158	*0.7*	172	11.02	26	8	23	17	0.3	0.70915
	Borgarfjörður	4	5	291	0.40	254.3	738.1	7.96	1.76	194	4.97	1745	*43*	532	637	131	*1.3*	166	11.02	23	8	30	17	0.4	n.a.
	Borgarfjörður	5	5	816	1.13	254.3	708.1	7.69	2.20	193	5.36	1793	*43*	556	640	*0*	*0.8*	172	11.41	14	10	25	17	1.3	n.a.
	Borgarfjörður	6	5	1632	2.27	254.3	678.1	7.76	2.40	183	5.22	1725	*39*	531	621	*0*	*0.9*	164	10.97	11	10	25	15	1.7	0.709164
	Borgarfjörður	7	5	3018	4.19	254.3	648.1	7.71	2.63	166	5.01	1643	*31*	501	591	*0*	*1.1*	154	10.29	10	9	33	15	2.0	n.a.
	Borgarfjörður	8	5	6042	8.39	254.3	618.1	7.71	2.89	170	5.27	1711	*33*	519	604	*0*	*1.2*	159	10.52	13	10	46	15	3.2	0.709152
	Hvítá	0	21	0	0	250.9	907.1	8.13	0.28	155	5.16	1546	181	447	455	*0*	*0.1*	130	8.85	*0*	7	39	13	3.4	0.709155
	Hvítá	1	21	22	0.03	250.9	877.1	7.18	1.87	113	4.55	1466	*16*	402	507	163	3.4	173	8.76	3	167	41	12	*0.1*	0.708753
	Hvítá	2	21	49	0.07	250.9	847.1	6.86	2.66	87	4.70	1528	*11*	414	519	218	3.7	152	8.81	*3*	212	41	12	*0.0*	0.708675
	Hvítá	3	21	92	0.13	250.9	817.1	6.74	3.24	80	5.05	1622	*4*	437	549	286	4.7	154	9.41	4	243	32	11	*0.0*	0.708609
	Hvítá	4	21	291	0.40	250.9	787.1	6.66	6.18	58	4.95	1602	*0*	431	548	508	6.5	154	9.35	*3*	257	33	8	*0.0*	0.708514
	Hvítá	5	21	816	1.13	250.9	757.1	6.65	5.24	44	4.88	1617	*4*	430	556	883	9.1	155	9.46	*2*	262	38	7	*0.0*	0.708424
	Hvítá	6	21	1632	2.27	250.9	727.1	6.65	5.94	30	4.71	1577	*8*	421	554	1258	11.1	151	9.26	5	258	44	5	*0.0*	0.708363
	Hvítá	7	21	3018	4.19	250.9	697.1	6.77	5.78	36	4.51	1530	*7*	408	540	1592	13.6	145	8.88	*2*	240	49	6	*0.0*	0.708352
	Hvítá	8	21	6042	8.39	250.9	667.1	6.84	4.79	18	4.52	1635	*1*	427	576	1989	10.6	149	9.52	4	244	41	6	*0.0*	0.708330
	Borgarfjörður	0	21	0	0	251.0	904.0	8.13	0.28	155	5.16	1546	181	447	455	*0*	*0.1*	130	8.85	*0*	7	39	13	3.4	0.709155
	Borgarfjörður	1	21	22	0.03	251.0	874.0	8.07	1.75	200	5.27	1679	104	538	587	176	*2.9*	214	11.10	20	11	28	19	*0.1*	n.a.
	Borgarfjörður	2	21	49	0.07	251.0	844.0	8.01	2.38	190	5.56	1718	*9*	547	600	181	*0.6*	191	11.01	19	12	22	18	*0.2*	n.a.
	Borgarfjörður	3	21	92	0.13	251.0	814.0	7.97	2.71	186	5.73	1738	*10*	557	601	105	*0.4*	185	10.92	17	11	25	16	0.4	0.709147
	Borgarfjörður	4	21	291	0.40	251.0	784.0	7.81	3.51	173	5.93	1728	*4*	553	584	35	*0.6*	183	10.71	16	10	22	18	0.8	n.a.
	Borgarfjörður	5	21	816	1.13	251.0	754.0	7.69	4.28	201	6.38	1813	*5*	581	620	*0*	*0.0*	189	11.22	13	14	22	16	1.3	n.a.
	Borgarfjörður	6	21	1632	2.27	251.0	724.0	7.67	4.92	192	6.35	1769	164	564	593	*0*	*2.4*	182	10.90	28	14	60	16	1.7	0.709151
	Borgarfjörður	7	21	3018	4.19	251.0	694.0	7.62	5.17	190	6.11	1681	86	527	569	*0*	*2.6*	174	10.35	15	14	41	15	2.1	n.a.
	Borgarfjörður	8	21	6042	8.39	251.0	664.0	7.59	4.59	172	6.08	1724	91	530	583	*0*	*0.7*	164	10.25	13	13	40	15	3.2	0.709171
Detection										14	0.04	0.01	46.3	1.8	4.9	0.01	3.0	1.2	0.31	3.3	1.4	3.2	0.9	0.3	
Maximum error (%)								0.05	0.02	14.6	2.27	2.3	>100	2.2	2.8	6.4	80.3	6.7	2.5	81.3	29.5	14.22	32.78	>100	0.000017

n.a.: denotes "not analyzed", italics denote concentrations below the detection limit.

saturation state of the reactive fluids with respect to selected minerals is provided in Electronic Supplement. The carbonate concentrations of these fluids were assumed to be in equilibrium with atmospheric CO_2 during the experiments. The majority of the primary minerals are undersaturated in the fluids. In the Hvítá bedload experiments at 5 and 21 °C, albite, anorthite, enstatite, forsterite, and K-feldspar all become more undersaturated with time, while diopside becomes less supersaturated. In the Borgarfjörður estuarine sediment experiments anorthite, enstatite, and forsterite remain undersaturated throughout the experiments and diopside remains supersaturated at both studied temperatures. Both albite and K-feldspar change from undersaturated to supersaturated with time during the Borgarfjörður estuarine sediment experiments. The carbonate minerals aragonite, calcite, dolomite, and strontianite all become undersaturated and the SiO_2 polymorphs chalcedony and quartz change from undersaturated to saturated in all experiments through time. Amorphous silica remains undersaturated.

Other minerals display a range of saturation states. In the Hvítá bedload experiments, chlorite, illite, imogolite, allophane, gibbsite, alunite, scolecite, and thomsonite all change from supersaturated to undersaturated at both studied temperatures, with kaolinite becoming less supersaturated and talc becoming more undersaturated. This is in sharp contrast to the Borgarfjörður estuarine suspended experiments, where alunite, gibbsite, chlorite, imogolite, allophane, kaolinite, scolecite, and thomsonite all remain saturated or supersaturated in the fluid phase at 5 and 21 °C. Illite and talc change from under- to supersaturated with time at both temperatures.

3.2. Impact of dissolution on reacted seawater isotopic compositions

The impact of particulate dissolution in seawater on marine isotopic compositions was assessed in these experiments

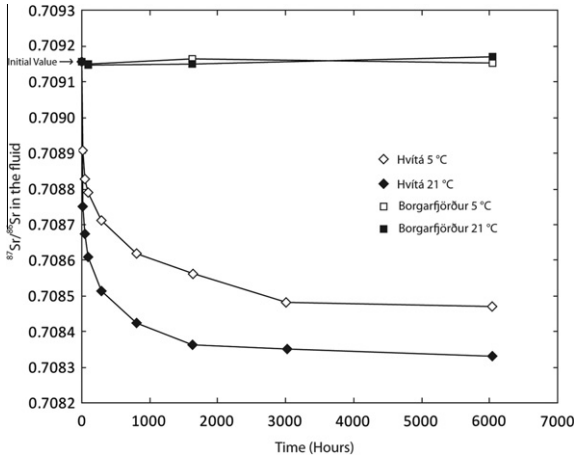

Fig. 4. The measured $^{87}Sr/^{86}Sr$ ratios in seawater after reaction with the particulate material. Each experiment had an initial measured seawater $^{87}Sr/^{86}Sr$ of 0.70916 (labeled on *y*-axis). The measured $^{87}Sr/^{86}Sr$ values of the particulate samples before the experiments were 0.7063 for the Borgarfjörður estuarine material and 0.7032 for the Hvítá bedload material. The errors are within the size of the symbols.

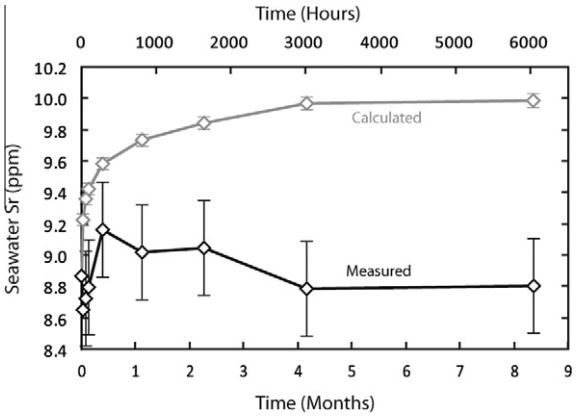

Fig. 5. A comparison of the measured Sr concentrations in seawater reacted with Hvítá bedload material at 5 °C with corresponding calculated Sr concentrations from the measured change in seawater $^{87}Sr/^{86}Sr$. This assumes no Sr is incorporated into secondary phases in the calculated concentrations. The error bars on the measured line are from uncertainty in ICP-MS measurements, the error bars on the calculated line are from uncertainties associated with measurements of $^{87}Sr/^{86}Sr$.

using the radiogenic Sr system. The evolution of $^{87}Sr/^{86}Sr$ in the reacted seawater is shown as a function of elapsed time in Fig. 4. The $^{87}Sr/^{86}Sr$ ratios of seawater reacted with the Hvítá bedload material decrease continuously with time. As the $^{87}Sr/^{86}Sr$ ratio of the original bedload material in these experiments is 0.70318 (relative to the original seawater $^{87}Sr/^{86}Sr$ ratio of 0.70916), and the total Sr concentration in the seawater is close to constant (Table 2), the observed temporal evolution of the reacted seawater $^{87}Sr/^{86}Sr$ ratio indicates the continuous two-way flux of Sr out of and into the solids. In contrast, the $^{87}Sr/^{86}Sr$ ratios of seawater reacted with the Borgarfjörður estuarine material remain relatively constant. The two-way flux of Sr from the riverine bedload can be due to (1) metal exchange, (2) adsorption, and/or (3) the dissolution of primary material and concurrent precipitation of Sr-bearing secondary phases. In all likelihood all three of these processes contribute. Assuming that the Sr released to seawater had the same $^{87}Sr/^{86}Sr$ ratio as the bulk particulate matter, the $^{87}Sr/^{86}Sr$ ratio of the reacted seawater can be calculated from the following mass balance relationship:

$$^{87}Sr/^{86}Sr_{fluid} = \frac{(m_{Sr,sw} \times {}^{87}Sr/^{86}Sr_{sw}) + (m_{Sr,solid} \times {}^{87}Sr/^{86}Sr_{solid})}{(m_{Sr,sw} + m_{Sr,solid})} \quad (1)$$

where $m_{Sr,sw}$ and $m_{Sr,solid}$ denote the mass of Sr contained in original seawater and that released from the solids, respectively. The suffixes *fluid*, *solid*, and *sw* after $^{87}Sr/^{86}Sr$ denote the isotopic ratio of the reacted seawater sample, original particulate material, and original seawater, respectively. Rearranging Eq. (1) yields:

$$m_{Sr,solid} = \frac{m_{Sr,sw}\left({}^{87}Sr/^{86}Sr_{sw} - {}^{87}Sr/^{86}Sr_{fluid}\right)}{\left({}^{87}Sr/^{86}Sr_{fluid} - {}^{87}Sr/^{86}Sr_{solid}\right)} \quad (2)$$

which provides an estimate of the total Sr released from the particulate material directly from the measured $^{87}Sr/^{86}Sr$

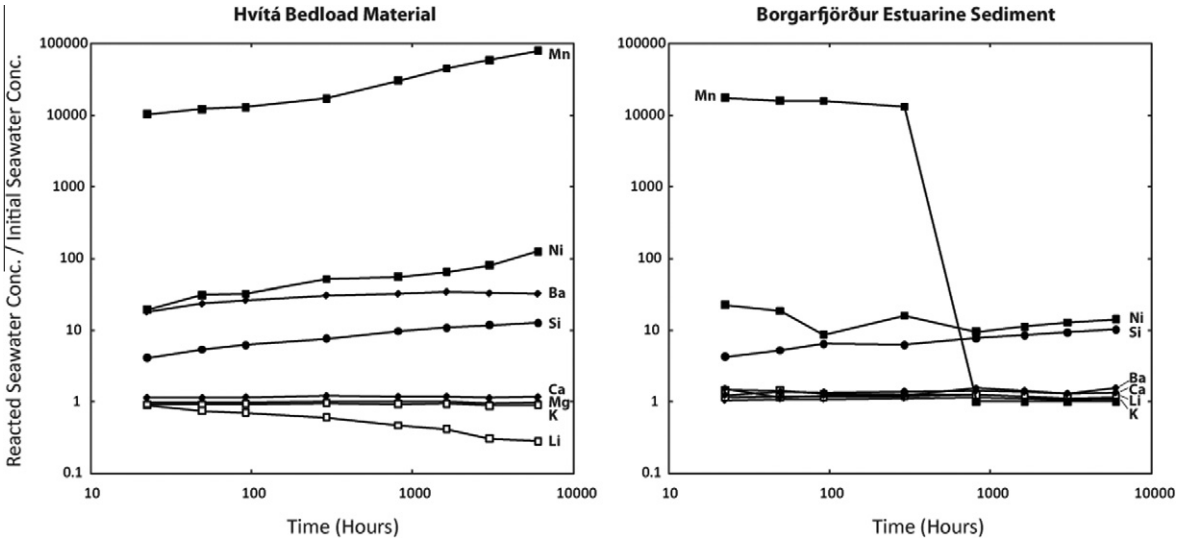

Fig. 6. The ratio of the concentration of selected elements relative to that of the initial seawater in the Hvítá bedload and the Borgarfjörður sediment experiment at 5 °C. The original seawater and final four Borgarfjörður reacted seawater Mn concentrations were below the detection limit of 0.01 ppb, so this detection limit was adopted for these solutions to calculate the ratios shown in this figure. Therefore, Mn ratios shown are likely to represent a lower limit of this ratio. The symbols match those described in the legend of Fig. 1.

ratio of the reacted seawater. Results of this calculation are shown in Fig. 5. Based on this calculation it is estimated that 3% of the total Sr present in this bedload material was released during the 9 month long experiment. This calculated flux is markedly different from the estimate ascertained by considering the variation of the total Sr content of the reacted seawater. In contrast, $^{87}Sr/^{86}Sr$ ratio analysis of the Borgarfjörður sediment dissolution experiments show that only a negligible fraction of the total original Sr contained in this solid was released to seawater in this experiment. Note that the calculations performed using Eqs. (1) and (2) are based on the assumption that the Sr released to the fluid has the same $^{87}Sr/^{86}Sr$ ratio as the bulk solid. This assumption is supported by the observation that there is only a minor difference in the $^{87}Sr/^{86}Sr$ ratios between coexisting glasses and feldspars in evolved volcanic rocks (Davies and Halliday, 1998) and therefore this difference should be negligible in basaltic rocks.

4. DISCUSSION

4.1. Comparison to natural system behavior

The experiments presented above indicate a significant difference between the chemical interactions of Hvítá bedload and the Borgarfjörður sediment with seawater. The degree to which this difference may be an artifact associated with the drying of the samples, one of which was recovered from fresh river water the other from saline estuary brine, prior to their use in the experiments can be assessed using mass balance calculations. The total mass of residual salts precipitated on the particulates during drying can be estimated assuming the particulate material has a porosity of 40%, consistent with a closed packed geometry and a density of 3 g cm^{-3}. Using the Hvítá River composition reported by Pogge von Strandmann et al. (2008b), mass balance calculations suggest that residual salts dissolution would have increased the Li, K, and Ca concentration of the reacted seawater during our experiments by 0.08 ppb, 0.13 ppm, and 1.06 ppm, respectively. This contrasts with the observed behavior of these elements, as Li and K decrease markedly, while Ca increases by 61–95 ppm, in the reacted seawater (Table 2). It seems likely therefore that residual salt dissolution was insignificant during these experiments. In contrast, parallel calculations indicate that residual salts precipitated on the Borgarfjörður estuarine material would result in an increase of 0.04 ppm Li, 392 ppm Mg, 0.3 ppm Si, 108 ppm K, 136 ppm Ca, and 2.3 ppm Sr in the reacted seawater. These values are comparable to that observed in the experiments for all these elements except Mg and Si, suggesting that the observed variation of Li, K, Ca, and Sr are dominated by the dissolution of residual salts. The extremely fast release of K, Mg, and Ca from the Borgarfjörður sediment (Fig. 3) supports the argument that these are due to readily dissolvable salts. This conclusion is validated by the negligible variation in reacted seawater $^{87}Sr/^{86}Sr$ ratio during the experiments despite the increase in Sr concentrations. In contrast, the Mg concentration increased less than and the Si concentration increased more than that suggested by the residual salt calculation. These calculations also indicated that the effect of residual salt dissolution was negligible for transition metals such as Mn and Ni.

Despite the likely effect of dissolved salts on the release rates of some of the elements from the Borgarfjörður estuarine material, the differences in behavior between the river and the estuary materials remain considerable. Fig. 6 shows the relative enrichments of elements in the seawater reacting with the Hvítá bedload material and Borgarfjörður estuarine material at 5 °C. The largest differences in behavior between the two samples after discounting for the contribution of dissolved salts are exhibited by Ba, Mn,

and Ni. The increases in Ba concentrations during the Borgarfjörður estuarine experiments are minimal, while the concentrations are over 30 times higher in the Hvítá bedload experiments than the initial fluid (Table 2). The metals Mn and Ni are released in both experiments but are much more so in the Hvítá bedload experiment. The increases in reacted seawater Mn concentrations shown in Fig. 6 are likely to be underestimates as the detection limit (0.01 ppb) was used as the value for the original seawater. The behavior of Mn in the Borgarfjörður experiments is noteworthy as concentrations only remain above the detection limit for about a month (see Table 2), suggesting that Mn is subsequently incorporated into a precipitating secondary phase that does not immediately begin to precipitate. A subsequent drop in seawater concentration is also observed for Si and Ni (see Fig. 3). While Si concentrations are elevated by more than an order of magnitude for all the experiments, the residual salt corrected release from Hvítá bedload material is greater by 25% than the corresponding Borgarfjörður sample (Table 2).

The observations summarized above suggest that the estuarine sediment's prior exposure to saline water has already led to some release, exchange, and/or precipitation of material in the estuary that has altered the reactivity of the particulate material. This conclusion is consistent with the behavior for the transition metals Cu, Cd, and Zn, whose dissolved concentrations reach peaks in dissolved concentrations in the middle part of another Icelandic estuary (Ólafsdóttir and Ólafsson, 1999). As Ca, Si, Ni, and Mn are essential nutrients required for marine primary production (Bruland et al., 1991), it is clear that the continuous arrival of riverine particulate material is fundamental to maintaining the vitality of near coastal ecosystems (Jeandel et al., 2011). Therefore, any change to sediment supply, either increasing through elevated soil erosion, or decreasing through damming, will have a significant impact on nutrient availability in coastal areas around basaltic terrains.

4.2. The potential role of basaltic particulate material dissolution to ocean chemistry

The behavior of Sr isotopes in this investigation is clear evidence for the substantial release of elements from riverine particulate material to the oceans. Experiments using Hvítá riverine bedload material exhibit a large change in seawater $^{87}Sr/^{86}Sr$ with little change in the total Sr concentrations. In contrast, the Borgarfjörður estuarine sediment experiments exhibit an increase in total Sr concentration and constant $^{87}Sr/^{86}Sr$ values around the starting value of 0.70916, suggesting that the Sr released to seawater originated from dissolved salts or the dissolution of phases precipitated in the estuary; negligible Sr originated from the dissolution of primary solids (Fig. 4 and Table 2). The difference in behavior between the riverine bedload and estuarine material from the same catchment is most logically accounted for by the prolonged contact of the latter with marine and brackish water prior to sampling, such that the Sr that is readily dissolvable/exchangeable from the estuarine particulate material has already been added to seawater. This is supported by the fact that the $^{87}Sr/^{86}Sr$ composition in the Borgarfjörður estuarine sediment is higher than the Icelandic riverine bedload material (Table 1). The percent of the total original Sr released from the Borgarfjörður estuarine sediment during its interaction with seawater can be estimated if it is assumed that the $^{87}Sr/^{86}Sr$ ratio of the Borgarfjörður sediment is a mixture of the original basaltic material and secondary phases with the same $^{87}Sr/^{86}Sr$ composition as seawater. Based on this hypothesis, 14.9% of Sr in the original basaltic material can be inferred to have been dissolved while interacting with estuarine waters.

The notable change in the seawater $^{87}Sr/^{86}Sr$ temporal evolution in the Hvítá experiments with little change in total dissolved Sr concentrations implies that there is either a rapid dissolution of Sr-bearing primary material ($^{87}Sr/^{86}Sr = 0.70318$) that is coupled to the formation of Sr bearing secondary phases, and/or that there is considerable exchange of Sr between the solid and fluid phases. Mass balance equations using Eq. (2) suggest that the Hvítá bedload material liberated 3.1% of its Sr, with much of this release occurring within the first 24 h of the experiments. The absence of contemporaneous increase in overall dissolved Sr concentrations (Fig. 5) strongly suggests that the Sr release from the Hvítá bedload material is coupled with the reverse flux of Sr into a solid phase.

The Sr isotopic system is not the only system to display variations within Borgarfjörður Estuary. Measurements of Li isotopes in suspended particulate matter show a linear relationship between δ^7Li and 1/[Li] (Pogge von Strandmann et al., 2008b), which suggests that suspended particles incorporate seawater Li into alteration minerals. Measurements of Mo isotope variations in the Borgarfjörður Estuary showed a dramatic drop in $\delta^{98/95}Mo$ at the mouth of the estuary below that of both the incoming dissolved $\delta^{98/95}Mo$ in the Hvítá River and seawater $\delta^{98/95}Mo$ values (Pearce et al., 2010). The authors suggested this was due to the release of isotopically light Mo adsorbed to particles or a change in redox conditions, consistent with the non-conservative behavior of U and the decrease in δ^7Li from the same samples (Pogge von Strandmann et al., 2008b). The measurements of Li, Mo, and U in this study each show decreases in dissolved seawater concentrations during the Hvítá bedload experiments and little change in the Borgarfjörður experiments (Table 2). This suggests that these elements may be adsorbed from seawater by incoming riverine particulates, or are incorporated into precipitating secondary phases upon arrival in the estuary, as observed for Sr in this study. As it is commonly assumed that riverine isotope composition is conservatively transferred to the ocean, the observed net sink of these elements into particulate phase has significant implications for the interpretation of the cycles of numerous elements.

The 3.1% Sr release from the Hvítá bedload material in seawater calculated from the change in $^{87}Sr/^{86}Sr$ using Eq. (2) suggests that basaltic particulate dissolution could be much greater than is evident from the changes in dissolved element concentrations. Note that this Sr release rate is likely independent of the fluid/solid ratio in our experiments, because the saturation states of most of the primary

minerals are strongly undersaturated. The fluid/solid ratio will, however, have an effect of the saturation state of secondary minerals, which will affect the degree to which released elements are reincorporated into the solid phase. The reactivity of the particulates in seawater is also evidenced by the increase of Si concentrations in all four experiments points, an observation complemented by light $\delta^{30}Si$ measurements indicative of basalt dissolution affecting $Si(OH)_4$ concentrations in waters around the basaltic island of Kerguelen in the Southern Ocean (Fripiat et al., 2011) and the long-held theory that silica in seawater is controlled by silicate minerals (Mackenzie et al., 1967). Other studies have observed that Nd isotopic compositions are dramatically affected by interaction with basaltic particulate material on continental margins (Lacan and Jeandel, 2005; Arsouze et al., 2009).

All of this evidence suggests that riverine particulate material dissolves to a significant extent once it arrives in the ocean and that this dissolution can have important consequences for global element fluxes. As can be seen in Fig. 1, particulate transport dominates dissolved riverine transport for the vast majority of elements globally. It follows from this figure that just a 1% release of an element from particulate material would mean that particulate material transport would be the primary riverine flux to the ocean for numerous elements including Fe, Al, Cr, and Zn, while being a considerable input of Si and Mn. Note that this 1% is considerably less than the 3% of the Sr released from the Hvítá bedload during the 9 month dissolution experiments presented above, and the 15% of the Sr released based on the relative Sr isotope composition of the riverine versus the estuarine particulate material. This suggests that the dissolution of basaltic particulate material in seawater may be an important and hitherto overlooked component of global element cycles. Results also indicate that a significant proportion of the mass dissolved into seawater is rapidly removed by the reincorporation into the solids. Although this process limits the degree to which the overall concentrations of elements in seawater are affected by the addition of particulate material, the dissolution of riverine transported particulates may greatly affect the isotopic composition of seawater.

5. CONCLUSION

The results summarized above demonstrate that riverine transported basaltic particulate material can significantly alter the composition of seawater upon their arrival to the ocean. Although the overall effect of this process is mitigated in terms of the total concentration of many major elements in seawater due to reincorporation into the solid phase, riverine transported basaltic material–seawater interaction appears to have a significant effect on two distinct processes:

(1) The release of numerous metal nutrients to near coastal waters: as riverine transported basaltic material–seawater interaction appears to provide a substantial quantity of these nutrients to reacted seawater, it can be concluded that anthropogenic influences such as increasing soil erosion and/or the damming of rivers, and variations in natural cycles such as soil formation or glaciations, could have an important effect on the ecosystem health of near coastal waters.

(2) The isotopic composition of seawater: the dissolution of primary particulate material has been demonstrated to influence strongly the $^{87}Sr/^{86}Sr$ ratio of reacted seawater. Mass balance calculations suggest that similar variations are likely for other isotopic systems. If such effects are shown to be general, riverine transported material–seawater interaction may prove to be a major contribution to isotopic mass balance in the global oceans.

ACKNOWLEDGEMENTS

We extend our thanks to Snorri Gudbrandsson and Haraldur Rafn Ingvason for sampling assistance, to Pierre Brunet for laboratory assistance, and to Catherine Jeandel for the provision of seawater. Sigurður Gislason, Catherine Jeandel, Philip Pogge von Strandmann, Bastien Georg and an anonymous reviewer kindly provided comments on an earlier version of this manuscript. Jeff Alt helpfully handled this manuscript. M.T. Jones and C.R. Pearce were supported by the EC Marie Curie 'MIN-GRO' Research and Training Network (MRTN-CT-2006-035488). M.T. Jones is currently supported by a Marie Curie Intra-European Fellowship (PIEF-GA-2009-254495).

APPENDIX A. SUPPLEMENTARY DATA

Supplementary data associated with this article can be found, in the online version, at doi:10.1016/j.gca.2011.10.044.

REFERENCES

Aller R. (1998) Mobile deltaic and continental shelf muds as suboxic, fluidized bed reactors. *Mar. Chem.* **61**, 143–155.

Aller R. C., Blair N. E. and Brunskill G. J. (2008) Early diagenetic cycling, incineration, and burial of sedimentary organic C in the central Gulf of Papua (Papua New Guinea). *J. Geophys. Res.* **113**, F01S09. doi:10.1029/2006JF000689.

Andersson P. S., Dahlqvist R., Ingri J. and Gustafsson O. (2001) The isotopic composition of Nd in a boreal river: a reflection of selective weathering and colloidal transport. *Geochim. Cosmochim. Acta* **65**, 521–527.

Arsouze T., Dutay J.-C., Lacan F. and Jeandel C. (2009) Reconstructing the Nd oceanic cycle using a coupled dynamical–biogeochemical model. *Biogeosciences* **6**, 1–18.

Berner R. A. (1990) Global CO_2 degassing and the carbon cycle – comment on Cretaceous Ocean Crust at DSDP site-417 and site-418 – carbon uptake from weathering vs. loss by magmatic outgassing. *Geochim. Cosmochim. Acta* **54**, 2889–2890.

Berner R. A., Lasaga A. C. and Garrels R. M. (1983) The carbonate–silicate geochemical cycle and its effect on atmospheric carbon-dioxide over the past 100 million years. *Am. J. Sci.* **283**, 641–683.

Bruland K. W., Donat J. R. and Hutchins D. A. (1991) Interactive influences of bioactive trace metals on biological production in oceanic waters. *Limnol. Oceanogr.* **36**, 1555–1577.

Burton K. W. and Vance D. (2000) Glacial–interglacial variations in the neodymium isotope composition of seawater in the Bay

of Bengal recorded by planktonic foraminifera. *Earth Planet. Sci. Lett.* **176**, 425–441.

Davies G. R. and Halliday A. N. (1998) Development of the Long Valley rhyolitic magma system: strontium and neodymium isotope evidence from glasses and individual phenocrysts. *Geochim. Cosmochim. Acta* **62**, 3561–3574.

De La Rocha C. L., Brzezinski M. A. and DeNiro M. J. (1997) Fractionation of silicon isotopes by marine diatoms during biogenic silica formation. *Geochim. Cosmochim. Acta* **61**, 5051–5056.

Dürr H. H., Meybeck M., Hartmann J., Laruelle G. G. and Roubeix V. (2009) Global spatial distribution of natural riverine silica inputs to the coastal zone. *Biogeosci. Discuss.* **6**, 1345–1401. doi:10.5194/bgd-6-1345-2009.

Eythorsson J. and Sigtryggsson H. (1971) The climate and weather of Iceland. *Zool. Iceland* **1**, 1–62.

Falkowski P. G. (1997) Evolution of the nitrogen cycle and its influence on the biological sequestration of CO_2 in the ocean. *Nature* **387**, 287.

Falkowski P., Barber R. and Smetacek V. (1998) Biogeochemical controls and feedbacks on ocean primary production. *Science* **281**, 200–206.

Fripiat F., Cavagna A.-J., Dehairs F., Speich S., André L. and Cardinal D. (2011) Silicon pool dynamics and biogenic silica export in the Southern Ocean, inferred from Si-isotopes. *Ocean Sci. Discuss.* **8**, 639–674.

Gaillardet J., Dupré B. and Allègre C. (1999) Geochemistry of large river suspended sediments: silicate weathering or recycled tracers? *Geochim. Cosmochim. Acta* **63**, 4037–4051.

Gaillardet J., Viers J. and Dupré B. (2003) Trace elements in river waters. In *Surface and Ground Water, Weathering, and Soils*, vol. 5 (ed. J. I. Drever) (eds. H. G. Holland and K. K. Turekian). Elsevier.

Gannoun A., Burton K. W., Vigier N., Gislason S. R., Rogers N. W., Mokadem F. and Sigfússon B. (2006) The influence of weathering process on riverine osmium isotopes in a basaltic terrain. *Earth Planet. Sci. Lett.* **243**, 732–748.

Georg R. B., Reynolds B. C., West A. J., Burton K. W. and Halliday A. N. (2007) Silicon isotope variations accompanying basalt weathering in Iceland. *Earth Planet. Sci. Lett.* **261**, 476–490.

Gislason S. R. and Oelkers E. H. (2003) The mechanism, rates, and consequences of basaltic glass dissolution: II. An experimental study of the dissolution rates of basaltic glass as a function of pH and temperature. *Geochim. Cosmochim. Acta* **67**, 3817–3832.

Gislason S. R., Arnórsson S. and Ármannsson H. (1996) Chemical weathering of basalt in SW Iceland: effects of runoff, age of rocks and vegetative/glacial cover. *Am. J. Sci.* **296**, 837–907.

Gislason S., Oelkers E. and Snorrason Á. (2006) Role of river-suspended material in the global carbon cycle. *Geology* **34**, 49–52.

Gislason S. R., Oelkers E. H., Eiriksdottir E. S., Kardjilov M. I., Gisladottir G., Sigfusson B., Snorrason A., Elefson S. Ó., Hardardottir J., Torssander P. and Oskarsson N. (2008) Direct evidence of the feedback between climate and weathering. *Earth Planet. Sci. Lett.* **277**, 213–222.

Gudbrandsson S., Wolff-Boenisch D., Gislason S. R. and Oelkers E. H. (2011) An experimental study of crystalline basalt dissolution from $2 \leqslant pH \leqslant 11$ and temperatures from 5 to 75 °C. *Geochim. Cosmochim. Acta* **75**, 5496–5509.

Gysi A. P. and Stefansson A. (2008) Numerical modelling of CO_2–water–basalt interaction. *Mineral. Mag.* **72**, 55–59.

Holland H. D. (1984) *The Chemical Evolution of the Atmosphere and Oceans*. Princeton University Press, Princeton, New Jersey.

Holland H. D. (2005) Sea level, sediments and the composition of seawater. *Am. J. Sci.* **305**, 220–239.

Huh Y., Chan L. H. and Edmond J. M. (2001) Lithium isotopes as a probe of weathering processes: Orinoco River. *Earth Planet. Sci. Lett.* **194**, 189–199.

Jeandel C., Peucker-Ehrenbrink B., Jones M. T., Pearce C. R., Oelkers E. H., Godderis Y., Lacan F., Aumont O. and Arsouze T. (2011) Ocean margins: the missing term for oceanic element budgets? *EOS, Trans. Am. Geophys. Union* **92**, 217–224.

Jones M. T. and Gislason S. R. (2008) Rapid releases of metal salts and nutrients following the deposition of volcanic ash into aqueous environments. *Geochim. Cosmochim. Acta* **72**, 3661–3680.

Kisakürek B., James R. H. and Harris N. B. W. (2005) Li and δ^7Li in Himalayan rivers: proxies for silicate weathering? *Earth Planet. Sci. Lett.* **237**, 387–401.

Koroleff F. (1976) Determination of silicon. In *Methods of Seawater Analysis* (ed. K. Grasshoff). Springer Verlag, New York.

Kump L. R., Brantley S. L. and Arthur M. A. (2000) Chemical weathering, atmospheric CO_2 and climate. *Ann. Rev. Earth Planet. Sci.* **28**, 611–667.

Lacan F. and Jeandel C. (2005) Neodymium isotopes as a new tool for quantifying exchange fluxes at the continent–ocean interface. *Earth Planet. Sci. Lett.* **232**, 245–257.

Mackenzie F. T. and Garrels R. M. (1966) Chemical mass balance between rivers and oceans. *Am. J. Sci.* **264**, 507–525.

Mackenzie F. T., Garrels R. M., Bricker O. P. and Bickley F. (1967) Silica in seawater: control by silica minerals. *Science* **155**, 1404–1405.

Meybeck M., Laroche L., Dürr H. and Syvitski J. (2003) Global variability of daily total suspended solids and their fluxes in rivers. *Global Planet. Change* **39**, 65–93.

Michalopoulos P. and Aller R. C. (1995) Rapid clay mineral formation in Amazon delta sediments: reverse weathering and oceanic elemental cycles. *Science* **270**, 614–617.

Milliman J. and Syvitski J. (1992) Geomorphic/tectonic control of sediment discharge to the ocean: the importance of small mountainous rivers. *J. Geol.* **100**, 525–544.

Mörner N.-A. and Etiope G. (2002) Carbon degassing from the lithosphere. *Global Planet. Change* **33**, 185–203.

Oelkers E. H. and Gislason S. R. (2001) The mechanism, rates, and consequences of basaltic glass dissolution: I. An experimental study of the dissolution rates of basaltic glass as a function of aqueous Al, Si, and oxalic acid concentration at 25 °C and pH = 3 and 11. *Geochim. Cosmochim. Acta* **65**, 3671–3681.

Oelkers E. H. and Gislason S. R. (2004) The role of suspended material in the chemical transport of eastern Icelandic rivers. In *Water–Rock Interaction* (eds. Wanty and Seal). Taylor and Francis Group, London, pp. 865–868.

Oelkers E. H., Gislason S. R., Eiríksdóttir E. S., Jones M. T., Pearce C. R. and Jeandel C. (2011) The role of riverine particulate material on the global cycles of the elements. *Appl. Geochem.* **26**, S365–S369.

Ólafsdóttir S. R. and Ólafsson J. (1999) Input of dissolved constituents from River Þjórsá to S-Iceland coastal waters. *Rit Fiskideildar* **16**, 79–88.

Parkhurst D. and Appelo C. (1999) User's guide to PHREEQC (version 2) – a computer program for speciation, batch-reaction, one-dimensional transport, and inverse geochemical calculations. *Water-Resource Investigation Report 99-4259*. US Geological Survey.

Pearce C. R., Burton K. W., Pogge von Strandmann P. A. E., James R. H. and Gislason S. R. (2010) Molybdenum isotope behaviour accompanying weathering and riverine transport in a basaltic terrain. *Earth Planet. Sci. Lett.* **295**, 104–114.

Peucker-Ehrenbrink B., Miller M. W., Arsouze T. and Jeandel C. (2010) Continental bedrock and riverine fluxes of strontium and

neodymium isotopes to the oceans. *Geochem. Geophys. Geosy.* **11**, Q03016. doi:10.1029/2009GC002869.

Pogge von Strandmann P. A. E., Burton K. W., James R. H., van Calsteren P., Gislason S. R. and Mokadem F. (2006) Riverine behaviour of uranium and lithium isotopes in an actively glaciated basaltic terrain. *Earth Planet. Sci. Lett.* **251**, 134–147.

Pogge von Strandmann P. A. E., Burton K. W., James R. H., van Calsteren P., Gislason S. R. and Sigfússon B. (2008a) The influence of weathering processes on riverine magnesium isotopes in a basaltic terrain. *Earth Planet. Sci. Lett.* **276**, 187–197.

Pogge von Strandmann P. A. E., James R. H., van Calsteren P., Gislason S. R. and Burton K. W. (2008b) Lithium, magnesium and uranium isotope behaviour in the estuarine environment of basaltic islands. *Earth Planet. Sci. Lett.* **274**, 462–471.

Pogge von Strandmann P. A. E., Burton K. W., Porcelli D., James R. H., Van Calsteren P. and Gislason S. R. (2011) Transport and exchange of U-series nuclides between suspended material, dissolved load and colloids in rivers draining basaltic terrains. *Earth Planet. Sci. Lett.* **301**, 125–136.

Raymo M. E., Ruddiman W. F. and Froelich P. N. (1988) Influence of the late Cenozoic mountain building on the ocean geochemical cycles. *Geology* **16**, 649–653.

Saemundsson K. (1979) Outline of the geology of Iceland. *Jökull* **29**, 7–28.

Stefánsdóttir M. and Gislason S. R. (2005) The erosion and suspended matter/seawater interaction during and after the 1996 outburst flood from the Vatnajökull Glacier, Iceland. *Earth Planet. Sci. Lett.* **237**, 433–452.

Stein M., Starinsky A., Katz A., Goldstein S. L., Machlus M. and Schramm A. (1997) Strontium isotopic, chemical, and sedimentological evidence for the evolution of Lake Lisan and the Dead Sea. *Geochim. Cosmochim. Acta* **61**, 3975–3992.

Syvitski J. (2003) Supply and flux of sediment along hydrological pathways: research for the 21st century. *Global Planet. Change* **39**, 1–11.

Syvitski J. (2011) Global sediment fluxes to the Earth's coastal ocean. *Appl. Geochem.* **26**, S373–S374.

Syvitski J., Peckham S., Hilberman R. and Mulder T. (2003) Predicting the terrestrial flux of sediment to the global ocean: a planetary perspective. *Sediment. Geol.* **162**, 5–24.

Tronnes R. G. (2003) *Introduction to the geology and geodynamics of Iceland*. Nordic Volcanological Institute.

Viers J., Dupré B. and Gaillardet J. (2009) Chemical composition of suspended sediments in World Rivers: new insights from a new database. *Sci. Total Environ.* **407**, 853–868.

Vigier N., Burton K. W., Gislason S. R., Rogers N. W., Duchene S., Thomas L., Hodge E. and Schaefer B. (2006) The relationship between riverine U-series disequilibria and erosion rates in a basaltic terrain. *Earth Planet. Sci. Lett.* **249**, 258–273.

Vigier N., Gislason S. R., Burton K. W., Millot R. and Mokadem F. (2009) The relationship between riverine lithium isotope composition and silicate weathering rates in Iceland. *Earth Planet. Sci. Lett.* **287**, 434–441.

Villiers S. D., Dickson J. A. D. and Ellam R. M. (2005) The composition of the continental river weathering flux deduced from seawater Mg isotopes. *Chem. Geol.* **216**, 133–142.

Vörösmarty C., Meybeck M., Fekete B., Sharma K., Green P. and Syvitski J. (2003) Anthropogenic sediment retention: major global impact from registered river impoundments. *Global Planet. Change* **39**, 169–190.

Walker J. C. G., Hays P. B. and Kasting J. F. (1981) A negative feedback mechanism for the long-term stabilization of Earth's surface temperature. *J. Geophys. Res.* **86**, 9776–9782.

Walling D. E. (2006) Human impact on land–ocean sediment transfer by the world's rivers. *Geomorphology* **79**, 192–216.

Wallmann K., Aloisi G., Haeckel M., Tishchenko P., Pavlova G., Greinert J., Kutterolf S. and Eisenhauer A. (2008) Silicate weathering in anoxic marine sediments. *Geochim. Cosmochim. Acta* **72**, 2895–2918.

White W. R. (2001) *Evacuation of Sediments from Reservoirs*. Thomas Telford Publishing, London.

Wimpenny J., James R. H., Burton K. W., Gannoun A., Mokadem F. and Gislason S. R. (2010) Glacial effects on weathering processes: new insights from the elemental and lithium isotopic composition of West Greenland rivers. *Earth Planet. Sci. Lett.* **290**, 427–437.

Wolff-Boenisch D., Gislason S. R., Oelkers E. H. and Putnis C. V. (2004) The dissolution rates of natural glasses as a function of their composition at pH 4 and 10.6, and temperatures from 25 to 74 °C. *Geochim. Cosmochim. Acta* **68**, 4843–4858.

Wolff-Boenisch D., Gislason S. R. and Oelkers E. H. (2006) The effect of crystallinity on dissolution rates and CO_2 consumption capacity of silicates. *Geochim. Cosmochim. Acta* **70**, 858–870.

Zhu Q., Aller R. C. and Fan Y. (2006) Two-dimensional pH distributions in bioturbated marine sediments. *Geochim. Cosmochim. Acta* **70**, 4933–4949.

Associate editor: Jeffrey C. Alt